Electron Acceleration by a Tightly Focused Laser Beam

Yousef I. Salamin* and Christoph H. Keitel†

Theoretische Quantendynamik, Fakultät für Physik, Universität Freiburg, Hermann-Herder Strasse 3, D-79104 Freiburg, Germany

(Received 20 July 2001; published 15 February 2002)

State-of-the-art petawatt laser beams may be focused down to few-micron spot sizes and can produce violent electron acceleration as a result of the extremely intense and asymmetric fields. Classical fifth-order calculations in the diffraction angle show that electrons, injected sideways into the tightly focused laser beam, get captured and gain energy in the GeV regime. We point out the most favorable points of injection away from the focus, along with an efficient means of extracting the energetic electron with a static magnetic field.

DOI: 10.1103/PhysRevLett.88.095005 PACS numbers: 52.38.Kd

Laser acceleration has been of continuous interest as a competitive mechanism to acceleration by expensive conventional means. It has recently been demonstrated [1], by numerical integration of the equations of motion, that a single electron, incident initially at some angle to the axis of a laser beam, may be captured and violently accelerated to GeV energies. Feasibility of such an acceleration configuration, involving reflection rather than capture, has also been demonstrated experimentally [2]. The renewed interest in this work is motivated by new strides [3] in the development of high-intensity laser systems which may eventually open the door for the construction of high-energy laser accelerators.

Most theoretical treatments of electron laser acceleration employ low-order Gaussian or Bessel beams [4]. The ultimate goal is obviously to reach GeV or even TeV energies, a task that requires the use of laser fields of extremely high intensity. Such intensities may be produced in the laboratory by focusing over extremely small spatial dimensions, typically a few microns. This calls for a detailed knowledge of the laser electric and magnetic fields near the beam focus. The question arises, in this connection, whether a field description based upon low-order Gaussian or Bessel beams is adequate. In addition to laser acceleration, there is also the interest in numerous novel effects occurring in ultraintense laser particle interactions for which this Letter may be relevant. Such effects include quantum electrodynamic corrections [5], laser induced fusion [6], and generation of coherent high-frequency light [7].

This Letter aims to accomplish three goals in addition to demonstrating that laser acceleration into the GeV regime is possible when the electron is injected at a small angle to the axis of the tightly focused laser beam. First, we show that focusing a laser beam to a few micron spot size requires inclusion of terms of fifth order in the diffraction angle ϵ in the description of the associated fields. Second, we demonstrate that initial injection of the electron towards points on the beam axis on both sides of the focus may lead to substantially more gain than if injected directly into the focus. Third, extraction of a captured electron is shown to be possible by means of a static laboratory magnetic field.

The beam shown in Fig. 1 may be modeled by a vector potential linearly polarized along $+x$ from which the following electric field components may be derived [8,9]

$$E_x = E\left\{S_0 + \epsilon^2\left[\xi^2 S_2 - \frac{\rho^4 S_3}{4}\right] + \epsilon^4\left[\frac{S_2}{8} - \frac{\rho^2 S_3}{4} - \frac{\rho^2(\rho^2 - 16\xi^2)S_4}{16} - \frac{\rho^4(\rho^2 + 2\xi^2)S_5}{8} + \frac{\rho^8 S_6}{32}\right]\right\}, \quad (1)$$

$$E_y = E\xi v\left\{\epsilon^2 S_2 + \epsilon^4\left[\rho^2 S_4 - \frac{\rho^4 S_5}{4}\right]\right\}, \quad (2)$$

$$E_z = E\xi\left\{\epsilon C_1 + \epsilon^3\left[-\frac{C_2}{2} + \rho^2 C_3 - \frac{\rho^4 C_4}{4}\right] + \epsilon^5\left[-\frac{3C_3}{8} - \frac{3\rho^2 C_4}{8} + \frac{17\rho^4 C_5}{16} - \frac{3\rho^6 C_6}{8} + \frac{\rho^8 C_7}{32}\right]\right\}. \quad (3)$$

Similarly, the magnetic field components are given by

$$B_x = 0, \quad (4)$$

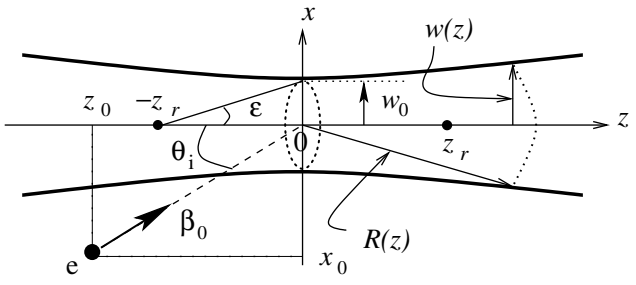

FIG. 1. The beam geometry. See text for the definitions.

$$B_y = E\Big\{S_0 + \epsilon^2\Big[\frac{\rho^2 S_2}{2} - \frac{\rho^4 S_3}{4}\Big] + \epsilon^4\Big[-\frac{S_2}{8} + \frac{\rho^2 S_3}{4} + \frac{5\rho^4 S_4}{16} - \frac{\rho^6 S_5}{4} + \frac{\rho^8 S_6}{32}\Big]\Big\}, \quad (5)$$

$$B_z = E\upsilon\Big\{\epsilon C_1 + \epsilon^3\Big[\frac{C_2}{2} + \frac{\rho^2 C_3}{2} - \frac{\rho^4 C_4}{4}\Big] + \epsilon^5\Big[\frac{3C_3}{8} + \frac{3\rho^2 C_4}{8} + \frac{3\rho^4 C_5}{16} - \frac{\rho^6 C_6}{4} + \frac{\rho^8 C_7}{32}\Big]\Big\}. \quad (6)$$

Note that a cross section through the beam focus is circular and has a radius w_0; a cross section through an arbitrary point z on axis is also circular with a radius given by $w(z) = w_0\sqrt{1 + (z/z_r)^2}$. With $k = 2\pi/\lambda$, the Rayleigh length is $z_r = kw_0^2/2$ and the diffraction angle is $\epsilon = w_0/z_r$. In Eqs. (1)–(6), $\xi = x/w_0$, $\upsilon = y/w_0$, and

$$E = E_0\,\frac{w_0}{w}\exp\Big[-\frac{r^2}{w^2}\Big]; \qquad E_0 = kA_0\,, \quad (7)$$

$$S_n = \Big(\frac{w_0}{w}\Big)^n \sin(\psi + n\psi_G); \qquad n = 0, 1, 2, \ldots, \quad (8)$$

$$C_n = \Big(\frac{w_0}{w}\Big)^n \cos(\psi + n\psi_G)\,. \quad (9)$$

Furthermore, $k = \omega/c$, $r^2 = x^2 + y^2$, and $\rho = r/w_0$. These equations were derived from a vector potential with an amplitude A_0 and a frequency ω. Also, $\psi = \psi_0 + \psi_P - \psi_R + \psi_G$, where ψ_0 is a constant phase, $\psi_P = \eta = \omega t - kz$ is the plane wave phase, $\psi_G = \tan^{-1}(z/z_r)$ is the Guoy phase associated with the fact that a Gaussian beam undergoes a total phase change of π as z changes from $-\infty$ to $+\infty$, $\psi_R = kr^2/(2R)$ is the phase associated with the curvature of the wave fronts, and $R(z) = z + z_r^2/z$ is the radius of curvature of a wave front intersecting the beam axis at the coordinate z. The fields given above satisfy Maxwell's equations $\nabla \cdot \boldsymbol{E} = 0 = \nabla \cdot \boldsymbol{B}$, plus terms of order ϵ^6.

We discuss the dynamics of the electron, of mass m, and of charge $-e$, by numerically solving the equations

$$\frac{d\boldsymbol{p}}{dt} = -e[\boldsymbol{E} + \boldsymbol{\beta} \times \boldsymbol{B}], \qquad \frac{d\mathcal{E}}{dt} = -ec\boldsymbol{\beta} \cdot \boldsymbol{E}\,. \quad (10)$$

In Eqs. (10) the quantities have their usual definitions: the momentum $\boldsymbol{p} = \gamma mc\boldsymbol{\beta}$, the energy $\mathcal{E} = \gamma mc^2$, the Lorentz factor $\gamma = (1 - \beta^2)^{-1/2}$, and the velocity, normalized by the speed of light c in vacuum, is $\boldsymbol{\beta}$. The *peak* field intensity I_0 will be expressed in terms of $q = eE_0/mc\omega$, where $I_0\lambda^2 \approx 1.375 \times 10^{18} q^2$ $(\mathrm{W/cm^2})\,(\mu\mathrm{m})^2$.

We will consider projection of the trajectories onto the plane of polarization. Without any loss of generality, the electron, in all the examples to be considered, will be fired from the point whose Cartesian coordinates are $(x_0, 0, z_0)$ towards a point on the beam axis a distance s from the focus. For our purposes in this Letter we will take, as *the boundaries* of the beam, the curves in the xz plane defined by $x = \pm w(z)$. An electron will be *transmitted* if its trajectory crosses the line $x = w(z)$, it will be considered *reflected* if the trajectory crosses the line $x = -w(z)$ twice. Otherwise, it will be considered *captured* by the beam. Strictly speaking, the field intensity on the curves $x = \pm w(z)$ falls down to $1/e^2$ of its maximum value on axis. Thus a transmitted or reflected electron will be weakly affected by the laser fields beyond the beam boundaries.

Figure 2(a) illustrates the three distinct cases of electron motion following injection towards the focus of the beam. In Figs. 2(b) and 2(c) the variation of E_x and E_z, respectively, along the electron trajectories are shown. Two oscillations with substantial asymmetry are apparent in 2(b) and the correlation between them and the trajectory oscillations is quite evident, especially in the case of capture.

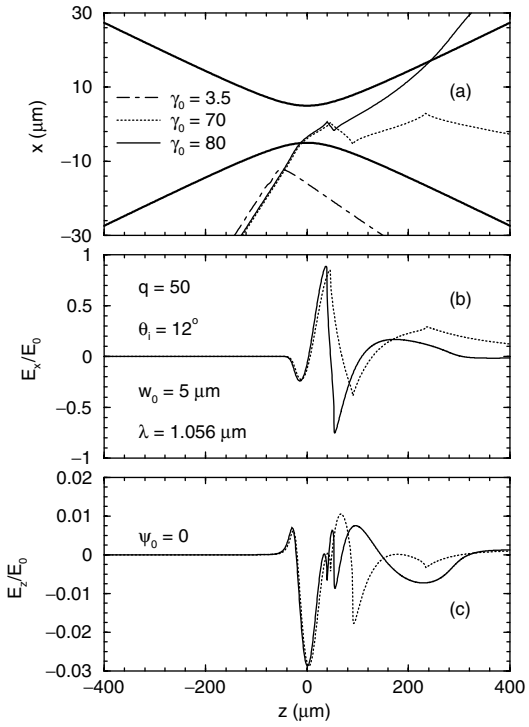

FIG. 2. (a) Portions of trajectories illustrating reflection, capture, and transmission, when the electron is injected into the focus. The dark lines mark the beam *boundaries* as defined in the text. (b) The transverse component, and (c) the longitudinal component of the electric field sensed by the electron along the transmission and capture trajectories displayed in (a). For all cases, $z_0 = -3$ mm, and peak intensity $I_0 \approx 3.08 \times 10^{21}$ W/cm^2. The *full* interaction time is such that $\omega t = \pi \times 10^5$, at the end of which the gains are ≈207 MeV (capture), ≈40 MeV (transmission), and ≈25 MeV (reflection). The legends in (a) apply to (b) and (c).

We recall that this asymmetry in the tightly focused regime is essential, because, according to the Lawson-Woodward theorem, in a symmetric plane wave where every *accelerating* half cycle is followed by an equally *decelerating* one, no net gain is to be expected [10].

Note that E_z is roughly 2 orders of magnitude smaller than E_x; yet, together with the $\boldsymbol{\beta} \times \boldsymbol{B}$ force, it contributes significantly to the forward drift and to the rate at which the electron gains energy from the field, as can be inferred from Eq. (10). Only a small portion of the actual trajectory is shown in Fig. 2(a). The energy gains reported here (see the caption to Fig. 2) are the ones found at the very end point on each trajectory. Still, it should be noted that the transfer of momentum takes place over a small portion of the trajectory in the nature of a series of impulses delivered mainly by the $\boldsymbol{\beta} \times \boldsymbol{B}$ and E_z forces. After that the electron mostly follows a straight line path at $\beta \rightarrow 1$.

Next we show that terms of order up to ϵ^5 in the field description are essential. To this end, the energy gain, defined as $(\gamma - \gamma_0)mc^2$, is shown versus the beam waist radius at focus in Fig. 3. Three distinct regions show up in Fig. 3(a). R_1 corresponds to spot sizes of radii $w_0 > 20\ \mu$m, for which all corrections that go as ϵ^2 and smaller may be dropped. The inset shows substantial gain for large ω_0 once the beam boundary approaches the electron's initial position. Since we kept the maximal laser intensity constant, rather than the laser power, the large w_0 values require very high laser powers prior to focusing, and are thus of little practical significance. In R_2, of radii roughly $7\ \mu\text{m} < w_0 < 20\ \mu$m, the terms of order ϵ^5 represent small corrections to the terms of order ϵ^3. However, in R_3 where $w_0 < 7\ \mu$m, inclusion of terms up to ϵ^5 seems to be essential, for the given parameter set. Our calculations with this particular set, the results of which are not shown, indicate that the terms of order ϵ^5 represent but tiny corrections to the terms of order up to ϵ^4, down to $w_0 \approx 4\ \mu$m. Thus, for $w_0 < 20\ \mu$m higher than first order corrections in ϵ are necessary for our parameter regime; up to fifth-order corrections appear sufficient down to and probably even well below $w_0 = 4\ \mu$m.

In Fig. 3(b) we investigate the role of the constant phase ψ_0 introduced in Eqs. (8) and (9) which alters the fields and the final energy in a sensitive way. For example, the fields sensed by the electron along its trajectories display a high degree of symmetry, in the sense described above, for ψ_0 values roughly in the range from 60° to 90°. Thus, for the chosen parameter set, such fields result in virtually no energy gain. Elsewhere in Fig. 3(b) the reverse is true, i.e., lack of field symmetry leads to substantial energy gain.

Obviously, the fields are strongest near the beam focus. However, the high-field region is very small and highly symmetric. This allows for a short interaction time, provided the electron is initially energetic enough to penetrate the focal spot. This means an electron that is aimed directly at the focus may easily get transmitted with little energy change, if at all. Slightly to the right of the focus, the beam is thicker and less symmetric. This allows for more interaction time and facilitates capture and high energy gain, as can be seen in Fig. 4.

Energy gains of a few hundred MeV have, thus far, been reported for laser intensities of a few times 10^{20} W/cm^2.

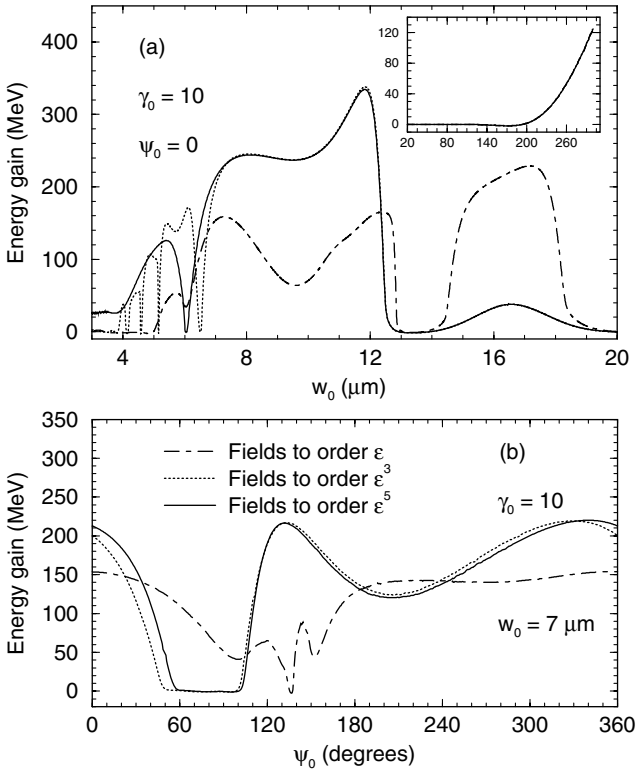

FIG. 3. For injection at $\theta_i = 6°$ into the focus, we show variation of the gain with: (a) The beam waist radius at focus w_0, and (b) the constant phase angle ψ_0. The laser wavelength is $\lambda = 1\ \mu$m and its peak intensity is $I_0 \approx 5.5 \times 10^{20}$ W/cm^2 ($q = 20$). The initial electron coordinates are ($x_0 = z_0 \tan\theta_i$, 0, $z_0 = -3$ mm) and its injection kinetic energy is $K = 4.599$ MeV. The interaction time is such that $\omega t = \pi \times 10^5$. The legends in (b) apply to (a), as well.

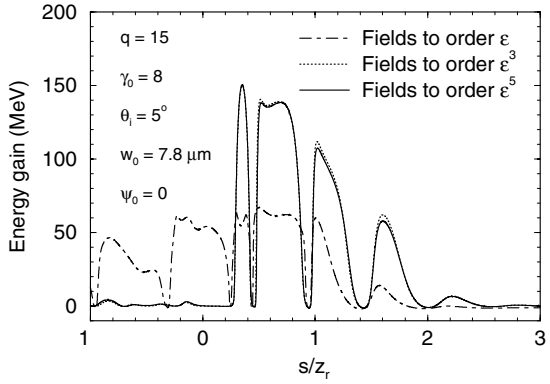

FIG. 4. Variation of the energy gain with s when contributions to the fields of order up to ϵ^N, $N = 1$, 3, and 5, are taken into account. The electron initial position is $[x_0 = -(s - z_0)\tan\theta_i, 0, z_0 = -3$ mm] and it is injected into the point $(0, 0, s)$. The laser wavelength is $\lambda = 1\ \mu$m, and its peak intensity is $I_0 \approx 3.09 \times 10^{20}$ W/cm^2. The interaction time is such that the plane-wave phase η changes by $4\pi \times 10^3$.

In Fig. 5, at an intensity near the ultimate currently achievable [3] and with somewhat larger injection energies, we find electron energy gains in the GeV regime. For example, injection at $K_i \approx 3.69$ MeV [see 5(e) for the other parameters] results in capture and an energy gain of about 1.589 GeV. A static magnetic field of strength 5 T, applied in the $-y$ direction over the small region $6 < z < 9.2$ cm, suffices to bend the electron trajectory and cause it to cross the beam boundary, as may be seen in Figs. 5(c), 5(d), and 5(e). As the electron changes course, it suffers inelastic collisions with the photons that would otherwise stream by, and loses about 5% of the gained energy. For a different choice of the parameter set, the electron may even gain, rather than lose energy in the process. Alternatively, extraction may be possible using a parabolic mirror, with a high enough damage threshold, to diffract the beam away, letting the electrons pass through a hole [11].

Our model employs monochromatic fields, while ultraintense pulses tend to possess a significant bandwidth, which, in turn, leads to sensitive phase variations whose effect eventually propagates to influence the electron energy gain. To illustrate this point, we have calculated the energy gained by a single electron under the conditions of Fig. 5(e) for frequencies in a band of width $\Delta\nu = 1.136\,363 \times 10^{12}$ Hz, centered on $\nu_0 = c/\lambda = 2.840\,909 \times 10^{14}$ Hz. The results are displayed in Fig. 5(f). It can be inferred from these data that contribution from all frequencies roughly in the band $\nu_0 \pm 0.14\%$ will enhance the gain, while those slightly outside will lower it, but not substantially.

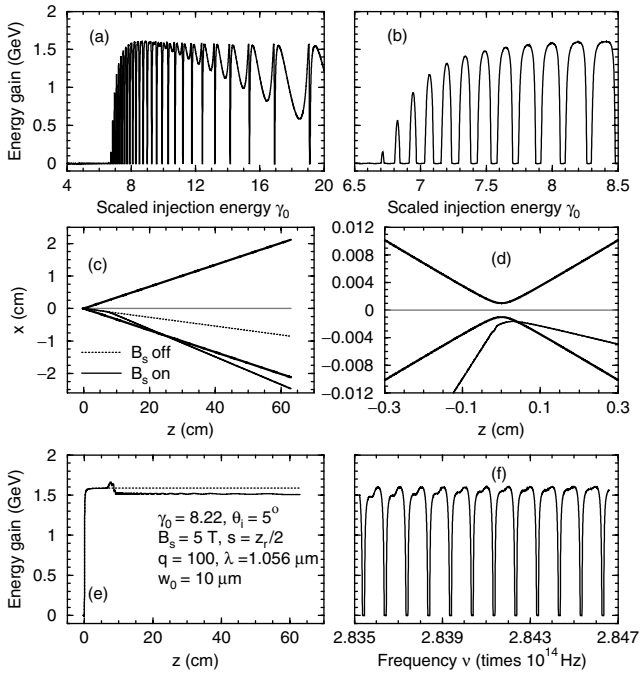

FIG. 5. (a) and (b) Energy gain vs the scaled injection energy γ_0. The peak field intensity is $I_0 \approx 1.375 \times 10^{22}$ W/cm^2. (c) and (d) Actual trajectories of the electron with and without B_s. (e) Gain accompanying the motion displayed in (b). (f) Gain for the example shown in (e) vs the laser frequency. The parameters given in (e) and the legends in (c) apply everywhere.

In conclusion, the electron dynamics in a tightly focused intense laser beam of a few micron spot size is adequately described via an analysis including up to fifth-order terms in the diffraction angle. The adjustable injection parameters have been optimized in order to take advantage of maximal intensity and asymmetry of the fields. GeV electrons are shown to be extracted by a static magnetic field after off-focus injection.

Y. I. S. acknowledges support from the German DAAD Gastdozentenprogramm. C. H. K. is funded by the German Science Foundation (Nachwuchsgruppe within SFB 276).

*Permanent address: Physics Department, Birzeit University, P.O. Box 14, Birzeit, West Bank, Palestinian Authority.
Electronic address: salamin@physik.uni-freiburg.de
†Electronic address: keitel@physik.uni-freiburg.de

[1] J. X. Wang *et al.,* Phys. Rev. E **58**, 6575 (1998); L. J. Zhu, Y. K. Ho, J. X. Wang, and L. Feng, J. Phys. B **32**, 939 (1999); Q. Kong *et al.,* Phys. Rev. E **61**, 1981 (2000); Y. Cheng and Z. Z. Xu, Appl. Phys. Lett. **74**, 2116 (1999); P. X. Wang *et al.,* Appl. Phys. Lett. **78**, 2253 (2001).

[2] P. H. Bucksbaum, M. Bashkansky, and T. J. McIlrath, Phys. Rev. Lett. **58**, 349 (1987); C. I. Moore, J. P. Knauer, and D. D. Meyerhofer, Phys. Rev. Lett. **74**, 2439 (1995); G. Malka and J. L. Miquel, Phys. Rev. Lett. **77**, 75 (1996); G. Malka, E. LeFebvre, and J. L. Miquel, Phys. Rev. Lett. **78**, 3314 (1997); K. McDonald, Phys. Rev. Lett. **80**, 1350 (1998); P. Mora and B. Quesnel, *ibid.* **80**, 1351 (1998).

[3] M. D. Perry *et al.,* Opt. Lett. **24**, 160 (1999); J. Andruszkow *et al.,* Phys. Rev. Lett. **85**, 3825 (2000); Th. Stöhlker *et al.,* Phys. Rev. Lett. **86**, 983 (2001); M. Drescher *et al.,* Sci. Expr. 1058561 (2001).

[4] B. Hafizi, A. Ting, E. Esarey, P. Sprangle, and J. Krall, Phys. Rev. E **55**, 5924 (1997); B. Hafizi, A. K. Ganguly, A. Ting, C. I. Moore, and P. Sprangle, Phys. Rev. E **60**, 4779 (1999); F. V. Hartemann *et al.,* Phys. Rev. E **58**, 5001 (1998); Y. I. Salamin and C. H. Keitel, Appl. Phys. Lett. **77**, 1082 (2000); Y. I. Salamin and F. H. M. Faisal, Phys. Rev. A **61**, 043801 (2000); Y. I. Salamin, F. H. M. Faisal, and C. H. Keitel, Phys. Rev. A **62**, 053809 (2000); H. Hora, Nature (London) **333**, 337 (1988).

[5] C. Bula *et al.,* Phys. Rev. Lett. **76**, 3116 (1996).

[6] T. Ditmire *et al.,* Nature (London) **398**, 489–492 (1999).

[7] S.-Y. Chen, A. Maksimchuk, E. Esarey, and D. Umstadter, Phys. Rev. Lett. **84**, 5528 (2000); K. Z. Hatsagortsyan and C. H. Keitel, Phys. Rev. Lett. **86**, 2277 (2001).

[8] L. W. Davis, Phys. Rev. A **19**, 1177 (1979); J. P. Barton and D. R. Alexander, J. Appl. Phys. **66**, 2800 (1989); K. T. McDonald, www.hep.princeton.edu/~mcdonald/accel/gaussian.ps and accel/gaussian2.ps

[9] M. O. Scully and M. S. Zubairy, Phys. Rev. A **44**, 2656 (1991).

[10] K. McDonald and K. Shmakov, Phys. Rev. ST Accel. Beams **2**, 121301 (1999); E. Esarey, P. Sprangle, and J. Krall, Phys. Rev. E **52**, 5443 (1995).

[11] J. L. Hirshfield and C. Wang, Phys. Rev. E **61**, 7252 (2000).